

Optical spectra of the heavy fermion uniaxial ferromagnet UGe₂

V. Guritanu,¹ N. P. Armitage,^{1,2} R. Tediosi,¹ S. S. Saxena,³ A. Huxley,⁴ and D. van der Marel¹

¹*Département de Physique de la Matière Condensée, Université de Genève, quai Ernest-Ansermet 24, CH 1211 Genève 4, Switzerland,*

²*Department of Physics and Astronomy, The Johns Hopkins University, Baltimore, MD 21218, USA*

³*Department of Physics, Cavendish Laboratory, University of Cambridge, Madingley Road, Cambridge CB3 0HE, United Kingdom*

⁴*Scottish Universities Physics Alliance, School of Physics, University of Edinburgh, Edinburgh EH9 3JZ, United Kingdom*

(Received 14 June 2008; revised manuscript received 1 October 2008; published 21 November 2008)

We report a detailed study of UGe₂ single crystals using infrared reflectivity and spectroscopic ellipsometry. The optical conductivity suggests the presence of a low-frequency interband transition and a narrow free-carrier response with strong frequency dependence of the scattering rate and effective mass. We observe sharp increase in the low-frequency mass and reduction in scattering rate below the upper ferromagnetic transition $T_C=53$ K indicating the emergence of a heavy fermion state triggered by the ferromagnetic order. The characteristic changes are exhibited most strongly at an energy scale below 12 meV. They recover their unrenormalized value above T_C and for $\omega > 40$ meV. In contrast no sign of an anomaly is seen at the lower transition temperature of unknown nature, $T_x \sim 30$ K, observed in transport and thermodynamic experiments.

DOI: [10.1103/PhysRevB.78.172406](https://doi.org/10.1103/PhysRevB.78.172406)

PACS number(s): 75.30.Mb, 71.27.+a, 78.20.-e

The possibility of unconventional superconductivity mediated by ferromagnetic fluctuations has long been a subject of theoretical speculation.^{1,2} Interest in this subject has been recently piqued with the discovery of superconductivity coexisting with the ferromagnetic state of UGe₂ under pressure.³ UGe₂ is a strongly anisotropic uniaxial ferromagnet with partially filled $5f$ electron states. Due to correlations and conduction band- $5f$ hybridization, carrier masses are found to be strongly enhanced⁴ $[(10-25)m_0]$ although specific-heat coefficients still fall an order of magnitude short of the largest values found in antiferromagnetic uranium-based heavy fermion (HF) compounds. UGe₂ exhibits a Curie temperature that strongly decreases with increasing pressure from about 53 K at ambient pressure to full suppression around 16 kbar. Superconductivity exists in a pressure region from 10 to 16 kbar, just below the complete suppression of ferromagnetism.³ Although superconductivity and ferromagnetism are usually found to be antagonistic phenomena, the observation fits within the now common scenario of finding superconductivity near the zero-temperature termination of a magnetic phase. In this sense it seemed quite natural to associate the superconductivity with being mediated by the magnetic fluctuations that diverge at a quantum critical point (QCP) perhaps as in the case of pressure driven superconductivity in the antiferromagnetic HF superconductors. However, the paramagnetic to ferromagnetic transition is strongly first order and is not associated with a peak in the effective electronic mass or superconducting transition temperature. It therefore appears that superconductivity is not directly related to the quantum phase transition connecting the ferromagnetic and paramagnetic states.^{5,6}

In addition to the main ferromagnetic transition, there appears to be an additional weak first-order transition of more enigmatic origin at lower temperatures (for $p=0$, $T_x=30$ K and for $T=0$, $p_x \approx 12.5$ kbar), which has been identified via resistivity,^{5,7,8} magnetization,⁶ and heat capacity.^{7,8} The critical pressure p_x is very close to that where the superconducting temperature is maximum, and it may be that the superconductivity is mediated via fluctuations from this weak first-order transition. The exact nature of the state below T_x is

not clear at present. It has been suggested that these two magnetic phases are related by a first-order Stoner-type phase transition in the spin magnetization due to a sharp double peak in the density of states near E_F .⁹ An alternative suggestion is that a competition between spin-orbit coupling and crystal-field effects drives a change in the local-moment configuration.¹⁰ Other possibilities such as a coexisting charge-density wave or spin-density wave order exist, however neutron scattering has failed to detect any such phases thus far.⁵ We also note that at ambient pressure the signatures of the lower transition T_x is only weakly visible in the resistivity¹¹ and magnetization measurements.^{6,12} Moreover, there is also no or almost no anomaly in the specific heat at ambient pressure.^{5,8} It may be that this transition at T_x does not extend all the way to zero pressure and, in fact, the line of first-order transitions terminates in a critical end point at finite temperature and pressure. T_x at ambient pressure is then indicative of a crossover and not a true phase transition.

In this Brief Report we present the results of a detailed optical study of UGe₂ single crystal using infrared reflectivity and spectroscopic ellipsometry. We have found a renormalized zero-frequency mode with a large frequency-dependent effective mass and scattering rate below the upper ferromagnetic transition T_C . They recover their unrenormalized values above T_C and for $\omega > 40$ meV. In contrast no sign of an anomaly is seen at $T_x \sim 30$ K. In the ferromagnetic state, we find signatures of a strong coupling to the longitudinal magnetic fluctuations which have been proposed to mediate unconventional superconductivity in this compound.

Measurements were performed in the frequency range from 6 meV to 3.7 eV combining infrared (IR) reflectivity via Fourier transform spectroscopy and ellipsometry from the near-infrared to ultraviolet energy range. The absolute value of the reflectivity $R(\omega, T)$ was calibrated against a reference gold layer evaporated *in situ* on the sample surface. Ellipsometry and IR data were combined using a Kramers-Kronig consistent variational fitting procedure.¹³ This allows the extraction over a broad energy range of all the significant frequency-dependent and temperature-dependent optical

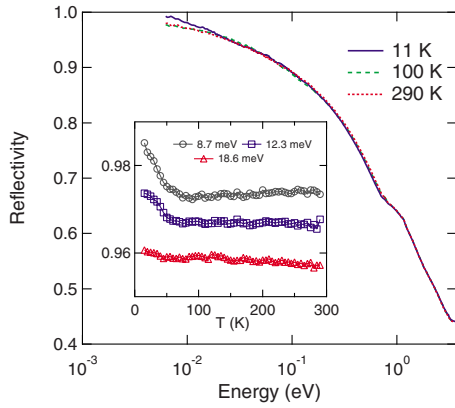


FIG. 1. (Color online) The normal-incidence reflectivity $R(\omega)$ of UGe_2 at three temperatures. The inset shows $R(\omega)$ at 8.7, 12.3, and 18.6 meV. The reflectivity curves at 100 and 290 K overlap on this scale.

properties such as, for instance, the complex conductivity $\sigma(\omega, T) = \sigma_1 + i\sigma_2$. The sample used for this Brief Report was grown at the CEA, Grenoble by the Czochralski technique.³ Measurements were taken in quasinormal incidence to the ac plane using linearly polarized light. We found only a small shift of the spectra between the two crystal directions with any differences smaller than our experimental accuracy (1%). The displayed spectrum is the average of the two directions.

Figure 1 shows the reflectivity spectra $R(\omega)$ over the full energy range. At high temperature $R(\omega)$ exhibits a monotonic increase as expected for a metal with $R(\omega) \rightarrow 1$ as $\omega \rightarrow 0$. As the sample is cooled below T_C the reflectivity shows a significant increase with the largest effects at low frequency (see Fig. 1 inset). No sign of an anomaly is found at the temperature T_x , which may be not surprising considering its weak signature in transport and thermodynamics at ambient pressure. It is interesting to mention that URu_2Si_2 also has a magnetic transition of unknown nature at low temperatures, which appears very pronounced in the infrared spectrum.¹⁴ The fact that in UGe_2 we see no signature of the second magnetic transition in the optical spectra, suggesting a very different nature of this transition in the two materials.

We observe that the reflectivity has no significant temperature dependence above 0.12 eV, which suggests a negligible temperature dependence at even higher frequencies. We used therefore room-temperature ellipsometry for frequencies greater than 0.74 eV to calculate the complex optical conductivity over the entire spectral range displayed in Fig. 2(a). We assign the peak at approximately 1 eV to an interband transition. At high temperature the low-frequency optical conductivity $\sigma_1(\omega)$ shows a broad Drude-type behavior as expected for a metal. The low-frequency conductivity is strongly temperature and frequency dependent. To clarify this trend we show an enlargement of the low-frequency data in Fig. 2(b). Several remarkable low-frequency structures form at low temperatures out of the broad Drude peak, including a very narrow zero-frequency mode which represents the intraband response of the heavy quasiparticles. The presence of a narrow zero-frequency mode is born out by two independent pieces of evidence: First, the imaginary part of

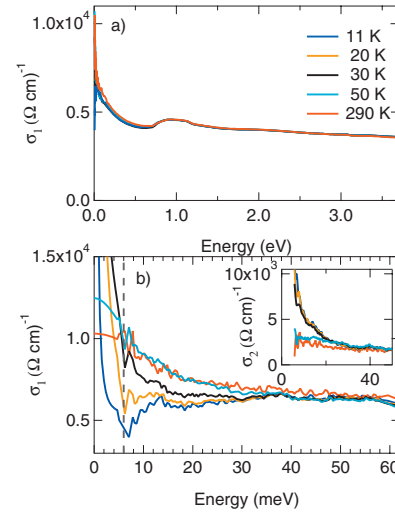


FIG. 2. (Color) (a) $\sigma_1(\omega)$ at different temperatures in the energy range of 0–3.7 eV. (b) The enlargement of the low-energy data including the zero-frequency extrapolations. The inset shows $\sigma_2(\omega)$ at different temperatures.

$\sigma(\omega)$ [see inset Fig. 2(b)] rises sharply when temperature is lowered below T_C . This implies a strong increase in metallic screening originating from the zero-frequency mode below the 6 meV threshold of the reflectivity data. The second piece of evidence is that comparing the dc resistivity¹⁵ at 11 and 290 K, $\sigma_1(\omega=0)$ increases by a factor of 48. This ratio is very close to the extrapolated conductivity ratio $\sigma_1(\omega \rightarrow 0, 11 \text{ K}) / \sigma_1(\omega \rightarrow 0, 290 \text{ K}) = 50$. This proves that there is really a narrow zero-frequency mode in the optical spectra at low temperatures. Concomitantly, a maximum develops at 13.6 meV and a weak structure at 37 meV. As will be shown below, these features reflect various aspects of the coherent HF and ferromagnetic states.

In order to further analyze the shape of the low-frequency spectra we use the extended Drude model. In this formalism the optical constants are expressed in terms of a frequency-dependent effective mass $m^*(\omega)/m$ and scattering rate $1/\tau(\omega)$ by the following expression:

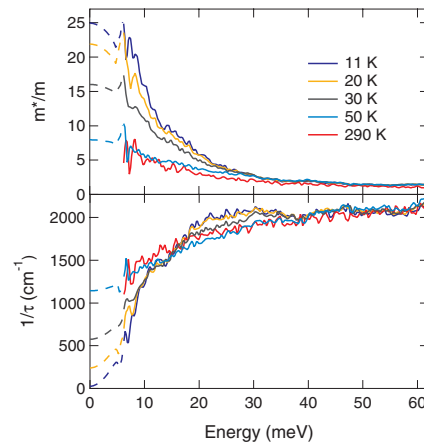


FIG. 3. (Color) The effective mass and the scattering rate as a function of photon energy derived from the extended Drude model with $\hbar\omega_p = 3.5$ eV. The dashed lines below 6 meV show the extrapolation toward zero frequency obtained as described in the text.

$$\frac{m^*(\omega)}{m} = -\frac{\omega_p^2}{4\pi\omega} \text{Im} \left[\frac{1}{\sigma(\omega)} \right], \quad \frac{1}{\tau(\omega)} = \frac{\omega_p^2}{4\pi} \text{Re} \left[\frac{1}{\sigma(\omega)} \right], \quad (1)$$

where $\hbar\omega_p = \sqrt{4\pi n e^2 / m_b} = 3.5$ eV is the total Drude plasma frequency and $\sigma(\omega)$ is the complex optical conductivity. $\hbar\omega_p$, which is determined through $m^*(\omega)/m=1$ at 290 K and $\omega=62$ meV, acts as a normalization constant and does not affect the trends as a function of ω and T .

Figure 3 displays the spectra of $1/\tau(\omega)$ and $m^*(\omega)/m$ as a function of frequency obtained from the extended Drude model for different temperatures. At room temperature both the scattering rate and the effective mass are nearly frequency independent. As the sample is cooled and the magnetic order develops the effective mass is strongly enhanced and the scattering rate suppressed. Such behavior suggests the development of heavy quasiparticles at low temperature. We observe that the strong increase in the effective mass and the rapid decrease in the scattering rate are largest below approximately 12 meV which can be regarded as the characteristic energy of the heavy quasiparticles. Below 6 meV we use the extrapolation toward zero frequency which gives a quasiparticle effective mass of over 25 for $\omega \rightarrow 0$ at the lowest T . Qualitatively this value is consistent with the cyclotron masses of (10–25) m_0 obtained by de Haas-van Alphen measurements.⁴

In Fig. 4 we present the temperature dependence of the effective mass and scattering rate at 0 and 8 meV obtained from Fig. 3. Note that at high temperature, in the paramagnetic state, both quantities are temperature independent. However, starting exactly at T_C the scattering rate becomes strongly suppressed and the effective mass enhanced. Such behavior contrasts with the usual situation in HF compounds, where mass renormalizations develop below a coherence temperature T^* different than the transition temperature to a magnetic state.¹⁶ Moreover, the conventional view is that the coherent HF state should actually be *suppressed* at a magnetic transition as the dominance of the Ruderman-Kittel-Kasuya-Yoshida (RKKY) interaction is expected to quench the Kondo effect.¹⁷ The observed behavior is not completely unprecedented; however, a number of other multi- f electron compounds have been found to undergo additional mass enhancements at the magnetic transition.¹⁶ In the present case however the magnetic transition appears to actually trigger the HF state suggesting an intrinsic $T^* < T_C$. This behavior may be related to multiple occupation of the $5f$ levels al-

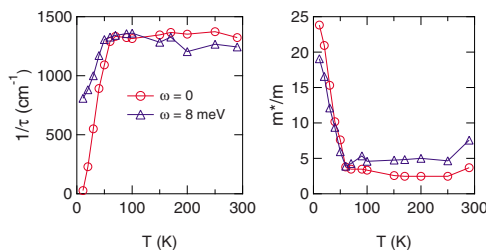


FIG. 4. (Color online) Temperature dependence of the effective mass and the scattering rate for two frequencies.

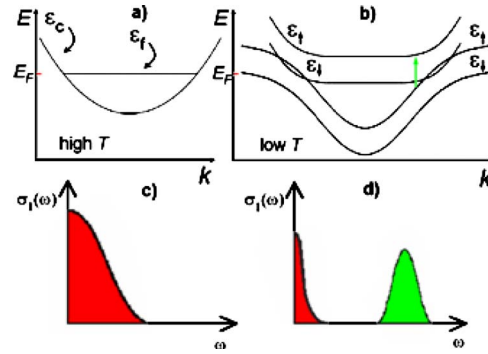


FIG. 5. (Color online) [(a) and (b)] Schematic band structure within the PAM of the conduction ϵ_c and the $5f$ electrons ϵ_f at high and low temperature, respectively. Vertical arrow indicates the interband transitions. ϵ_\uparrow and ϵ_\downarrow denote the spin-up and spin-down bands. [(c) and (d)] Sketch of the optical conductivity at high and low temperatures.

though we note that a similar effect in $3d$ electron systems has also been observed at the T_C of ferromagnetic $\text{Yb}_{14}\text{MnSb}_{11}$ (Ref. 18) and helimagnetic FeGe .¹⁹

The relatively large mass enhancement observed in UGe_2 suggests the evolution of renormalized itinerant charge carriers out of a Fermi gas coupled to a lattice of $5f$ local orbitals. It is generally accepted that the periodic Anderson model (PAM), which describes the hybridization of a localized level with a conduction band, captures the essential physics of such systems.^{20–22} In Fig. 5 we plot a schematic band dispersion of the PAM together with its optical conductivity at low and high temperature. At high T only a dispersive conducting band crosses the Fermi level (E_F), whereas the (partially filled) $5f$ bands at E_F are dispersionless. The intraband transitions give rise to a broad Drude conductivity sketched in Fig. 5(c). The additional scattering suppression which onsets at T_C implies a strong coupling between HF effects and magnetic ones with important implications for superconductivity. Therefore the occurrence of the HF and the ferromagnetic states cannot be explained using only the hybridization model; the effects of ferromagnetism have to be included. As the temperature is lowered, the material enters in a magnetically ordered state, which on one hand suppresses the channel for inelastic spin-flip scattering near E_F and on the other hand converts the $5f$ spin degrees of freedom into a narrow band of heavy charge carriers. This coherent band, partially occupied, and therefore pinned to E_F exhibits avoided crossings with the wide conduction bands due to hybridization. Excitations between the split bands create the possibility for new interband transitions [Fig. 5(b)] and redistribute spectral weight between high and low energies as shown in Fig. 5(d).

Although this general picture should hold in UGe_2 , additional features in principle are expected as a result of uranium's nominal $5f^3$ configuration which results in several $5f$ bands being involved in the heavy electron state. Moreover, as has been suggested for $\text{CeCo}_{1-x}\text{Ir}_x\text{In}_5$, a distribution of hybridization gaps due to a momentum dependence of the f - d coupling parameter^{23–25} may result in multiple features in $\sigma_1(\omega)$, such as seen in Fig. 2(b) at 37 and 13.6 meV.

The observed suppression in the scattering rate is addi-

tional to that expected generically for HF compounds below their coherence temperatures. The usual expectation is that the effective mass m^* and the quasiparticle lifetime τ^* are renormalized by approximately the same factor.²² In contrast, comparing the low-temperature scattering rates and masses with their high-temperature unrenormalized values we find the ratios $\frac{m^*}{m} \approx 6$ and $\frac{\tau^*}{\tau} \approx 50$, which disagree by a factor of 8. A similar analysis using instead the high-frequency values gives a similar discrepancy. It is also interesting to note that as the temperature increases the energy scale of the threshold in $1/\tau(\omega)$ does not appear to close at the transition, but instead the gap “fills in” and a remnant of this suppression persists even up to 290 K. Similar effects have been observed in ferromagnetic nickel.²⁶ This observation of gaps which fill in instead of closing is a common occurrence in strongly correlated systems.²⁷

In the optical spectra shown in Fig. 3 we observe a rather strong but incomplete suppression of $1/\tau(\omega)$ for frequencies smaller than about 6 meV. The suppression of the scattering rate, which onsets at T_C is reminiscent of that which occurs at energies below the Stoner gap in fully spin-polarized ferromagnets such as CrO_2 .²⁸ In such cases longitudinal Stoner-type spin-flip scattering is forbidden at energies below a threshold set by the energy difference from the bottom of the minority band to the Fermi level (the Stoner gap). UGe_2 is not fully spin polarized but has only a small minority spin population at E_F .^{29,30} Moreover, the behavior of properties such as the pressure-dependent magnetization and mechanisms of the pairing mechanism⁹ have been interpreted as a consequence of narrow peaks in the density of states, which could give an effective gap to spin-flip excitations. Such a density of states is supported by band calculations.¹⁰ Longitudinal fluctuations, which can possibly mediate exotic su-

perconductivity, have been found by neutron scattering.³¹ We note that conventional magnons are not expected to play a large role in a strongly uniaxial compound such as UGe_2 as their energy scales will be much higher. An effective gap to longitudinal spin-flip excitations has also been inferred through a Stoner model fit to the strength of magnetic Bragg peaks at low temperature with a gap that is on the order of the threshold in the optical scattering rate.³² It is interesting that our spectra give a strong indication of a coupling of charge to these longitudinal fluctuations that were originally proposed as a possibility to mediate superconductivity in ferromagnetic compounds.

Our observations suggest an interesting interplay between spin polarization and the HF coherent state. We believe that this is at the origin of the rather rich behavior of the optical conductivity resulting in two structures appearing below T_C (13.6 and 37 meV) and large quasiparticle renormalizations. The optical data indicate that the magnetic order triggers the transition into a state characterized by heavy and weakly scattered charge carriers. Our data are consistent with a strong coupling to the longitudinal magnetic modes which have been suggested to mediate superconductivity in this compound.

This work was supported by the Swiss National Science Foundation through Grant No. 200020-113293, the National Center of Competence in Research (NCCR) “Materials with Novel Electronic Properties-MaNEP,” and the European Science Foundation (ECOM-COST action P16). N. P. A. was partially supported through the NSF IRF program. The authors would like to thank N. Drichko, A. Kuzmenko, F. Lévy, J. A. Mydosh, and F. Ronning for helpful conversations and E. Koller for technical support.

-
- ¹V. L. Ginzburg, Sov. Phys. JETP **4**, 153 (1957).
²D. Fay *et al.*, Phys. Rev. B **22**, 3173 (1980).
³S. S. Saxena *et al.*, Nature (London) **406**, 587 (2000).
⁴Y. Ōnuki *et al.*, J. Phys. Soc. Jpn. **60**, 2127 (1991).
⁵A. Huxley *et al.*, Phys. Rev. B **63**, 144519 (2001).
⁶C. Pfleiderer *et al.*, Phys. Rev. Lett. **89**, 147005 (2002).
⁷C. G. Oomi *et al.*, J. Alloys Compd. **271-273**, 482 (1998).
⁸N. Tateiwa *et al.*, J. Phys. Soc. Jpn. **70**, 2876 (2001).
⁹K. G. Sandeman *et al.*, Phys. Rev. Lett. **90**, 167005 (2003).
¹⁰A. B. Shick *et al.*, Phys. Rev. B **70**, 134506 (2004).
¹¹G. Oomi *et al.*, Physica B (Amsterdam) **206-207**, 515 (1995).
¹²G. Motoyama *et al.*, Phys. Rev. B **65**, 020510(R) (2001).
¹³A. B. Kuzmenko, Rev. Sci. Instrum. **76**, 083108 (2005).
¹⁴D. A. Bonn *et al.*, Phys. Rev. Lett. **61**, 1305 (1988).
¹⁵Due to the irregular sample geometry the absolute value for the dc resistivity has not been obtained. Therefore the σ_{dc} values are not included in the fitting procedure.
¹⁶M. Dressel *et al.*, Phys. Rev. Lett. **88**, 186404 (2002).
¹⁷S. Doniach, Physica B & C **91**, 231 (1977).
¹⁸K. S. Burch *et al.*, Phys. Rev. Lett. **95**, 046401 (2005).
¹⁹V. Guritanu *et al.*, Phys. Rev. B **75**, 155114 (2007).
²⁰T. M. Rice *et al.*, Phys. Rev. B **34**, 6420 (1986).
²¹P. Fulde *et al.*, Solid State Phys. **41**, 1 (1988).
²²A. J. Millis *et al.*, Phys. Rev. B **35**, 3394 (1987).
²³K. S. Burch *et al.*, Phys. Rev. B **75**, 054523 (2007).
²⁴J. H. Shim *et al.*, Science **318**, 1615 (2007).
²⁵H. Weber *et al.*, Phys. Rev. B **77**, 125118 (2008).
²⁶D. E. Eastman *et al.*, Phys. Rev. Lett. **40**, 1514 (1978).
²⁷N. Furukawa, in *Physics of Manganites*, edited by T. Kaplan and S. Mahanti (Plenum, New York, 1999).
²⁸E. J. Singley *et al.*, Phys. Rev. B **60**, 4126 (1999).
²⁹A. B. Shick *et al.*, Phys. Rev. Lett. **86**, 300 (2001).
³⁰H. Yamagami, J. Phys.: Condens. Matter **15**, S2271 (2003).
³¹A. D. Huxley *et al.*, Phys. Rev. Lett. **91**, 207201 (2003).
³²N. Aso *et al.*, Phys. Rev. B **73**, 054512 (2006).